# Experimental and numerical analyses on determination of indirect (splitting) tensile strength of cemented paste backfill materials under different loading apparatus

Eren Komurlu [*1], Ayhan Kesimal [1a] and Serhat Demir [2b]

[1] *Department of Mining Engineering, Karadeniz Technical University, Trabzon, Turkey*
[2] *Department of Civil Engineering, Karadeniz Technical University, Trabzon, Turkey*

**Abstract.** The indirect tensile strengths (ITSs) of different cemented paste backfill mixes with different curing times were determined by considering crack initiation and fracture toughness concepts under different loading conditions of steel loading arcs with various contact angles, flat platens and the standard Brazilian test jaw. Because contact area of the ITS test discs developes rapidly and varies in accordance with the deformability, ITSs of curing materials were not found convenient to determine under the loading apparatus with indefinite contact angle. ITS values increasing with an increase in contact angle can be measured to be excessively high because of the high contact angles resulted from the deformable characteristics of the soft paste backfill materials. As a result of the change of deformation characteristics with the change of curing time, discs have different contact conditions causing an important disadvantage to reflect the strength change due to the curing reactions. In addition to the experimental study, finite element analyses were performed on several types of disc models under various loading conditions. As a result, a comparison between all loading conditions was made to determine the best ITSs of the cemented paste backfill materials. Both experimental and numerical analyses concluded that loading arcs with definite contact angles gives better results than those obtained with the other loading apparatus without a definite contact angle. Loading arcs with the contact angle of 15° was found the most convenient loading apparatus for the typical cemented paste backfill materials, although it should be used carefully considering the failure cracks for a valid test.

**Keywords:** tensile strength; indirect tensile strength test; splitting method; Brazilian test; paste backfill; finite element analyses

## 1. Introduction

The Brazilian test is the most popular indirect tensile strength (ITS) test method because it can be used with conventional compressive test equipment (Hobbs 1964, Barla and Innaurato 1973). The test is widely accepted to be invented by Prof. Fernando L.L.B. Carneiro (Carneiro 1943, Fairbairn and Ulm 2002), who was a very popular Brazilian concrete consultant. As an interesting event, Tsunei Akazawa, a Japanese scientist, independently developed splitting test and proposed

---

∗Corresponding author, Ph.D. Candidate, E-mail: ekomurlu@ktu.edu.tr
[a] Professor, E-mail: kesimal@ktu.edu.tr
[b] Ph.D. Candidate, E-mail: s.demir@ktu.edu.tr

the ITS determination method in the same year that Carneiro first announced his method (Akazawa 1943).

The Brazilian ITS ($\sigma_{tB}$) of rocks can be calculated using the Eq. (1), as suggested by International Society for Rock Mechanics (ISRM) (Ulusay and Hudson 2007)

$$\sigma_{tB} = -\frac{2P}{\pi dt} \tag{1}$$

where $d$ is the diameter of the disc specimen, $t$ is the thickness of the disc specimen and $P$ is the applied vertical load.

In the standard Brazilian test (splitting indirect tensile strength test), discs fail under biaxial stress conditions, including compressive radial stress ($\sigma_r$) along the vertical diameter and tangential stress ($\sigma_\theta$) along the horizontal diameter of the disc (Chen and Stimpson 1993, Fairhurst 1964, Krishnayya and Eisenstein 1974). The tangential tensile stress and compressive radial stress maximize at the center of the disc; thus, the crack initiation is expected to occur at the center of the disc. The maximum tensile stress can be calculated by using Eq. (1) derived from Muskhelishvili's equations that were suggested to estimate stress distribution in a disc diametrically compressed under a line load. Muskhelishvili (1963) suggested Eqs. (2)-(4) to calculate stress distribution in a disc diametrically compressed under a line load

$$\sigma_x = \frac{2P}{\pi t}\left(\frac{\sin^2\theta_1\cos\theta_1}{r_1} + \frac{\sin^2\theta_2\cos\theta_2}{r_2}\right) - \frac{2P}{\pi dt} \tag{2}$$

$$\sigma_y = \frac{2P}{\pi t}\left(\frac{\cos^3\theta_1}{r_1} + \frac{\cos^3\theta_2}{r_2}\right) - \frac{2P}{\pi dt} \tag{3}$$

$$\tau_x = \frac{2P}{\pi t}\left(\frac{\cos^2\theta_1\sin\theta_1}{r_1} + \frac{\cos^2\theta_2\sin\theta_2}{r_2}\right) \tag{4}$$

Geometric parameters of the Muskhelishvili equations are shown in Fig. 1. As the $\theta_1$ and $\theta_2$ in Eq. (2) are zero for a point on the vertical diameter of the disc, the tensile stress ($\sigma_x$) on vertical diameter can be calculated with Eq. (1). The suggested Brazilian ITS formula given in Eq. (1) is valid for the discs under linear diametral compressive loading. The classical theory assumes that the standard Brazilian jaws apply line load over a disc specimen with a high intensity (Hondros 1959). However, standard jaw contact with the disc specimen is not a line contact because of the curvilinear applied load over the circumference of the disc (Jaeger and Cook 1976). Standard Brazilian jaw is concave and has 8.1 cm arch diameter (Ulusay and Hudson 2007). Hondros (1959) analysed the Brazilian test for the case of a disc loaded by a uniform pressure applied radially over a short strip of the circumference at each end of the disc with definite contact angle ($2\alpha$). Hondros noted that the magnitude of $\alpha$ changes the stress distribution within disc directly. Because contact area of standard jaws varies in accordance with the disk material and contact angle is indefinite, use of the Hondros' approach is restricted for standard jaws and flat platens.

The tensile strengths of brittle materials like rock and concrete are generally much smaller than their compressive strengths. As the ratio of compressive strength to tensile strength ($\sigma_c/\sigma_t$) decreases, determination of the ITS of materials under diametral compressive loading appears
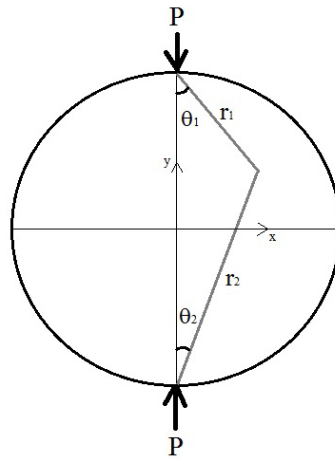
Fig. 1 Mesh grid of topographic model

to have a disadvantage due to possibility of crack initiation in the compression zone beneath the contact points (Fairhurst 1964). In addition, the friction conditions between the disc and jaws significantly affect the crack initiation and its position in a disc specimen (Kourkoulis *et al.* 2013).

The standard jaw does not make a line contact with the disc specimen because of the curvilinear load over the circumference of the disc. The contact area of the discs developes rapidly and varies in accordance with the disc and jaw materials (Jaeger and Cook 1976, Aono *et al.* 2012).

Although mode 1 (tensile) type cracks are expected to occur at the center of the Brazilian disc specimens, shear stresses can significantly change the failure load of randomly split discs due to the heterogeneity of the disc materials (Li and Aubertin 2002, Ulusay and Gokceoglu 1997, Ashour 1988). Systematic cracking follows the first crack initiation before the final failure occurs in a Brazilian ITS test. The difference between the failure and first crack initiation loads depends on the fracture toughness of the disc material. First crack stress, fracture toughness and failing mechanism of disc specimens are significantly influenced by the contact conditions. Ideal splitting for using Eq. (1) should initiate at the centre of the Brazilian disc, and cracks should propagate under the control of the tensile stresses along the vertical diameter. Stress distribution in a disc changes after the first crack occurrence. Stresses cannot be transmitted by discontinuities and immediately concentrate at the edges of cracks. The crack propagation resistance of a disc increases with an increase in contact angle (Erarslan and Williams 2012, Erarslan *et al.* 2012, Komurlu and Kesimal 2012).

The frictional stresses at the disc-jaw interface also change the stress distribution in the Brazilian test discs. Although the influence of friction at the center of a disc can be practically neglected when uniformly applied radial stress is created by the jaws, failure can begin in the compression zone due to the induced shear stresses beneath the loading platens. On the other hand, the influence of friction cannot be neglected for non-uniformly applied radial stress condition. Markides *et al.* (2012, 2010) and Kourkoulis *et al.* (2013) have reported detailed analyses on contact friction and its effect on stress distribution and deformations of discs under uniformly and non-uniformly distributed stresses. They suggested non-uniformly distributed radial stress conditions to better estimate the effect of the contact conditions on the stresses induced within the Brazilian test discs.

In recent years, researchers have started to investigate the use of loading arcs having same diameter with that of the disc tested and definite contact angle (Erarslan and Williams 2012, Komurlu and Kesimal 2015a). The researchers obtained more accurate results with steel arcs having definite contact angle than those observed when using standard jaws. However, the researchers reported that the contact angle changes the fracture toughness of the disc samples such that toughness increases with an increase in loading angle. Komurlu and Kesimal (2015a) reported that rock material properties especially deformation characteristics effect the determination of ITS of rock materials under various loading conditions, and ideal contact angle changes with the change of rock material. In this study, deformation characteristics of cemented paste backfill materials effect on the determination of the ITS is investigated with a series of Brazilian tests.

The novelty of this study is being first for using the loading arcs with definite contact angles to determine the ITS values of the cemented paste backfill materials. The aim of this study is to assess the effect of different loading geometries and contact angles on the validity of the Brazilian test and suggest a loading apparatus with a proper loading angle for typical cemented paste backfill materials used in mining. Material properties of a typical paste backfill mix are significantly different than those of rock materials or concretes with high cement content. Cement usage in a paste backfill material mix is to make the material filled in mine stopes stable under its self-weight and reinforce load bearing highly cemented rock-fill. Because cemented paste backfill are not generally applied as a support material, they are not designed to have a rock class strength, Modulus of Elasticity and brittleness (Komurlu *et al*. 2013, Komurlu and Kesimal 2015b, Emad *et al*. 2015, Kesimal *et al*. 2004, Yilmaz *et al*. 2015, 2011). Therefore, following the same testing procedure and details with those suggested for the rock and concrete materials with high cement contents can cause misleading determination of typical paste backfill materials ITS values of some hundreds kPa.

## 2. Experimental study

Series of ITS tests were carried out by using specimens with the diameter of NX size (5.47 cm). The discs were obtained from different paste backfill materials and tested under flat platens, standard jaw and $2\alpha = 15°$ and $2\alpha = 30°$ loading arcs.

The paste backfill materials used in this study were prepared by cementing mineral processing plant tailings of a Turkish copper mine with different cement ratios. The tailings comprises fine particles grinded by the mills of the plant: More than 70% of the tailings used in this experimental study had silt particle size (2 - 63 $\mu$m), and 10% of the tailings had clay (< 2 $\mu$m) particle size (Komurlu *et al*. 2013). There were two different types of material mixes prepared, which can be called as mixes with low and high cement ratios. The mix with low cement ratio was prepared as a paste backfill design which has 170 kg/m$^3$ Cem I type ordinary Portland cement, water to cement ratio of 235% by weight and 2110 kg/m$^3$ tailings. The mix with high cement ratio was designed to be a high strength paste backfill material including 400 kg/m$^3$ Cem I type ordinary Portland cement, water to cement ratio of 75% by weight, 1740 kg/m$^3$ tailings material, plasticizer with amount of 4% by weight of cement and accelerator with amount of 3% by weight of cement. Tap water was used in the mixes homogenized in a concrete mixer for 10 minutes. Then, the ITS test specimens were casted into NX size diameter molds with bottom allowing the bleed water drainage, compacted using tamping rods, and put on the vibration table to remove air in fresh mix (Fig. 2). A series of ITS tests was performed to determine the ITS values of paste backfill discs with 2, 5, 14 and 28 days curing time.

(a) Mixing          (b) Casting into molds          (c) Compaction using vibration table
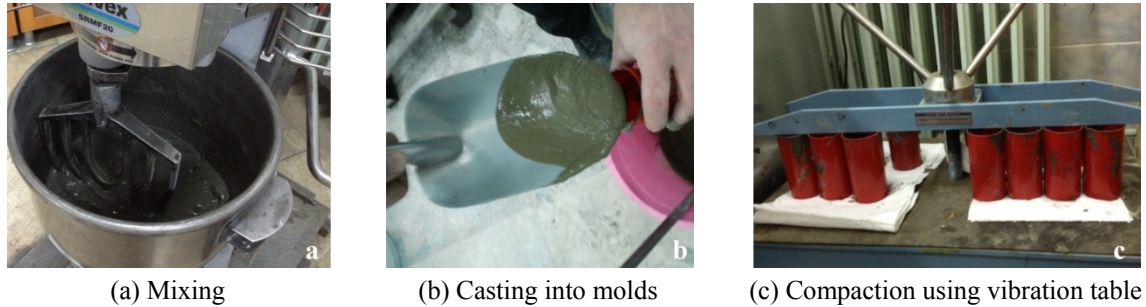
Fig. 2 Specimen preparation

Most of the discs loaded under the standard jaw were not ideally split through the centers of the disc specimens. In general, the scattered fractures were obtained under the standard Brazilian jaw. On the other hand, the discs under flat platens split with different shapes depending on the curing time. Discs with long curing times split along their vertical diameters. However, scattered cracks were observed from the soft discs with short curing time which were tested under the flat platen.

In general, the difference between the first crack initiation stress and the failure stress of the samples increased when the contact angle increased. When the discs were loaded with high contact angles, they were generally strangled and could not be easily split despite the occurrence of the first crack. To investigate the effect of thickness on the ITS values of the paste backfill materials, the test results and the thickness values of each specimens are given in Tables 1 and 2. The loading rate of the indirect tensile strength tests was respectively chosen 0.03 kN/sec and 0.1 kN/sec for specimens with low cement ratio and high cement ratio. Testing system used for the discs with low cement ratio has the loading capacity of 50 kN, which is a convenient system for testing low strength concrete, low strength rock and soil materials. Another press system with 200 kN load capacity was used for the discs with high cement ratio. The steel loading arcs were machined from standard milled steel, as recommended by ISRM (Fig. 3).

As seen from Table 3, failure load of the paste backfill specimens with high cement ratio under flat platens did not change with the curing time. Because 2 days curing discs were quite deformable, the contact area exceeded and caused to obtain unreliably high strength values. In contrast to discs with 14 days and 28 days curing time, discs with 2 and 5 days curing times showed several crack series under the flat platen (Figs. 4 and 6).
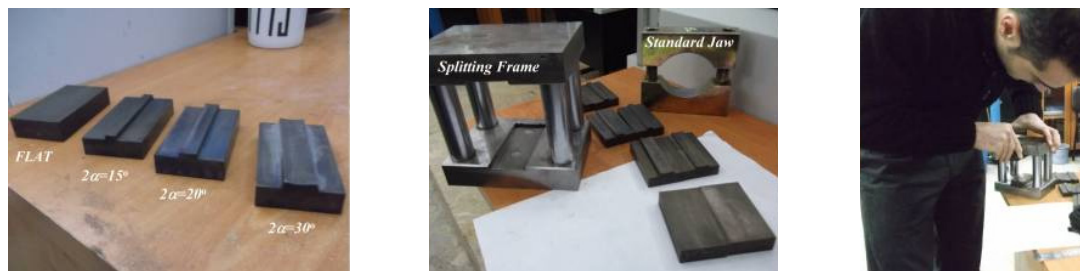


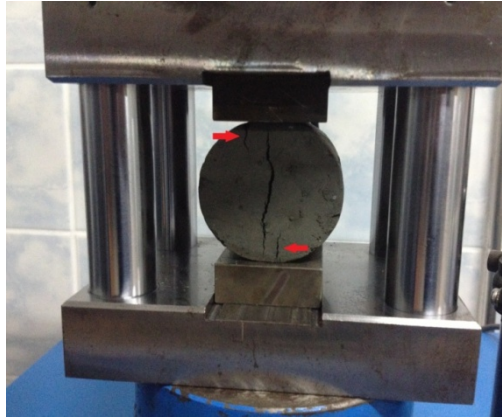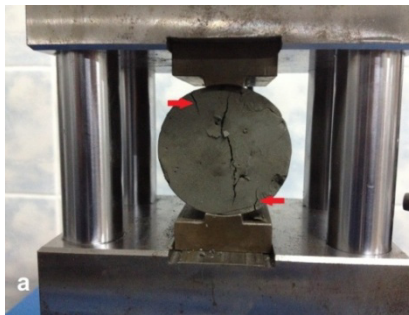Fig. 3 Testing apparatus and the steel loading arcs
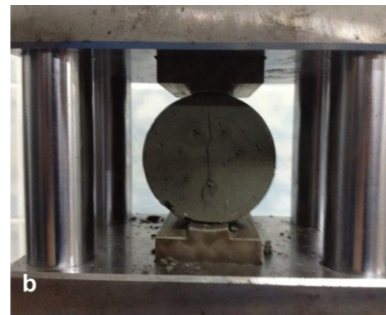
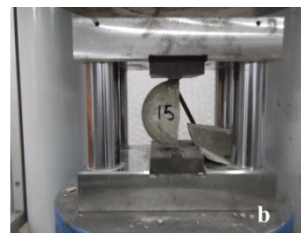Fig. 4 Five days cured disc under flat platen



|  (a)  |  (b)  |

Fig. 5 (a) 5 days; and (b) 28 days cured disc specimens with low cement ratio under 30° loading arcs



Fig. 6 Failed discs with high cement ratio under (a) flat platen; (b) 15° loading arc; (c)-(e) standard jaw

Table 1 ITS values of paste backfill specimens with high cement content

| Specimen type | Load type | $t$ (mm) | $\sigma_{tB}$ (MPa) |
|---|---|---|---|
| 14 days curing | SJ | 25 | 4.49 |
|  | SJ | 30 | 3.71 |
|  | SJ | 20 | 4.92 |
|  | 30° | 23 | 5.19 |
|  | 30° | 30 | 4.37 |
|  | 30° | 28 | 4.46 |
|  | 15° | 25 | 3.09 |
|  | 15° | 34 | 2.37 |
|  | 15° | 27 | 2.70 |
|  | Flat | 24 | 2.95 |
|  | Flat | 35 | 2.30 |
|  | Flat | 23 | 2.82 |
| 2 days curing | SJ | 31 | 2.72 |
|  | SJ | 33 | 2.65 |
|  | SJ | 25 | 3.07 |
|  | 30° | 27 | 3.05 |
|  | 30° | 32 | 2.59 |
|  | 30° | 30 | 2.32 |
|  | 15° | 34 | 1.91 |
|  | 15° | 27 | 2.24 |
|  | 15° | 31 | 2.02 |
|  | Flat | 35 | 2.64 |
|  | Flat | 29 | 2.27 |
|  | Flat | 28 | 3.15 |

The loading arcs let to obtain increase of strength measured with an increase in the curing time. Ideal central splitting shapes were obtained from the samples under 15° and 30° loading arcs (Fig. 6(b)). The standard Brazilian jaw caused different fracturing behaviors depending on the curing time of rock-like material. As the material was cured more and stiffened, several crack series were observed from the discs under the standard jaw. Fig. 6(c) shows specimens with 14 days curing time which failed under the standard jaw. Although discs with high cement ratio and curing time of 2 days failed with simple diametral cracks under standard jaw, significant differences between the first crack initiation and failure loads were obtained. This result again confirms the increase of toughness with an increase in contact angle. Fig. 6e shows failure of a disc with 2 days curing time which let 25% load increase after a major crack occurred under the standard jaw (Fig. 6(d)). Because of the excessive contact area of the highly deformable discs with 2 days curing time, split parts could not be migrated easily and load increase was permitted. The mean strength values of results measured from the test series are given in Table 3.

The branching of several fractures along the loading direction, under 30° loading arc was observed from the highly cemented past backfill specimens with the curing time of 14 days.

Table 2 ITS values of paste backfill specimens with low cement content

| Specimen type | Load type | $t$ (mm) | $\sigma_{tB}$ (MPa) |
|---|---|---|---|
| 14 days curing | SJ | 26 | 0.28 |
| | SJ | 31 | 0.28 |
| | SJ | 22 | 0.30 |
| | 30° | 22 | 0.36 |
| | 30° | 30 | 0.30 |
| | 30° | 29 | 0.27 |
| | 15° | 26 | 0.23 |
| | 15° | 32 | 0.20 |
| | 15° | 28 | 0.21 |
| | Flat | 30 | 0.19 |
| | Flat | 25 | 0.24 |
| | Flat | 28 | 0.22 |
| 2 days curing | SJ | 30 | 0.21 |
| | SJ | 32 | 0.22 |
| | SJ | 29 | 0.22 |
| | 30° | 28 | 0.19 |
| | 30° | 31 | 0.19 |
| | 30° | 29 | 0.20 |
| | 15° | 32 | 0.15 |
| | 15° | 26 | 0.16 |
| | 15° | 30 | 0.15 |
| | Flat | 25 | 0.20 |
| | Flat | 35 | 0.18 |

Similar splitting cracks along the loading direction were also observed from some specimens tested under the standard loading jaw. Because frequent crack series sometimes occurred following the central crack, an unexpected high amount of energy is believed to accumulate in the specimen due to the extensive contact area between the arcs and specimen when 30° loading arcs are used. On the contrary, specimens with high cement ratio and the curing time of 2 days did not shatter under the loading arcs and ideally split under 30° loading arcs. In contrast to the discs with high cement ratio, unexpected cracks near the edges of the 30° loading arcs were detected from the specimens with low cement ratio and curing time of 5 days after the central crack initiation (Fig. 5).

In general, multiple crack series occurred following the central crack of soft specimens with two days curing time discs under the flat platens. However, harder, more cured discs with the high cement ratio tested in this study failed with one central crack or a few narrow cracks. Discs with low cement ratio and 5 days curing time let the load increase, although the complete splitting crack through the vertical diameter occurred. Because of having high contact area under the flat platen, new cracks were induced to occur in the contact zone before failure (Fig. 4).

The paste backfill disc specimens showed various failure characteristics under the flat platens, standard Brazilian jaw, and the loading arcs with various angles. Failure load and the deformation

Table 3 Mean ITSs for the specimens tested under different loading types
(PBH: Paste backfill with high cement ratio, PBL: Paste backfill with low cement ratio)

| Specimen | SJ | Flat | 15° | 30° |
|---|---|---|---|---|
| PBH (2 days) | 2.81 | 2.69 | 2.06 | 2.65 |
| PBH(14 days) | 4.37 | 2.69 | 2.72 | 4.67 |
| PBL (5 days) | 0.22 | 0.19 | 0.15 | 0.19 |
| PBL (28 days) | 0.29 | 0.22 | 0.21 | 0.31 |

of the discs were found to be dependent on the loading type. In addition, the responses of the same material mixes under the same loading conditions also differed due to differences in their curing time.

## 3. Numerical modeling study

A series of Finite Element Analyses (FEM) was performed by using ANSYS software to better understand the stress distribution within a disk specimen under different loading apparatus. Eight-node solid brick elements (Solid65) were used for three-dimensional modeling of paste backfill materials, which have the capability of cracking in tension, crushing in compression, plastic deformation, and three degrees of freedom at each node, including transition in the nodal $x$, $y$, and $z$ directions. Materials were modeled by considering the linear and non-linear properties defining the behaviors of the elements. The elasticity modulus in model was assumed same for the tension and compression. The modeled materials were defined as linear elastic material until the crack initiation occurs. After the crack initiation, change of the tensile and shear stresses has been re-calculated by the program. The re-calculated shear stresses were transferred by the plasticity due to the generated open and closed cracks. The shear transfer coefficient was accepted as 0.3 and 0.1 for closed and open cracks, respectively. In addition, the stiffness reduction factor considered as 0.6 to define plasticity had an important role in the behavior of cracked elements.

This model predicted the failure of brittle materials according to the Willam–Warnke failure criteria used for concrete, rocks and other cohesive-frictional materials, such as ceramics (Willam and Warnke 1974). Material of loading apparatus was modeled with Solid185 as rigid steel with 400 GPa modulus of elasticity. The contact surfaces between the discs and loading apparatus were simulated with the Conta174 and Targe170 contact pairs. The friction coefficient between paste backfill materials and steel of the loading apparatus was considered as 0.3 for all analyses. Various loading apparatus of standard jaw, flat platen, 15° loading arc, 30° loading arc were modeled as shown in Fig. 7.

A static analysis was performed for each of the models, and the full Newton–Raphson method was used for non-linear analysis. For displacement-controlled loading, loads were divided into multiple substeps until the total load was achieved. Stress distributions and cracking mechanisms for all specimen models were plotted for comparison with the experimental results. Input parameters of the various material models are given in Table 4. The disc models had the diameter of NX core size and two different thickness to diameter ratios of 0.5 and 0.8. The mesh length in the disc models was chosen as 0.036 times the diameter.

Several representative figures for the stress distribution in discs under various loading conditions are given in Figs. 8-15. The stress distributions shown in the figures are for the discs
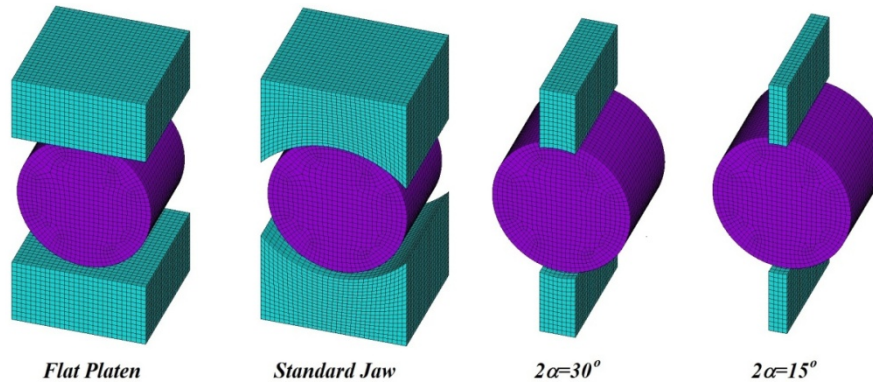
Fig. 7 Numeric models for the various loading apparatus

Table 4 Input parameters for disc models

| Model name | $\sigma_c$ (MPa) | $\sigma_t$ (MPa) | $E$ (GPa) | $v$ |
|---|---|---|---|---|
| Model 1 | 40 | 4 | 20 | 0.25 |
| Model 2 | 4 | 0.4 | 2 | 0.25 |
| Model 3 | 1 | 0.1 | 0.5 | 0.20 |

Table 5 ITS values calculated for the numerical models

| Model type | $t/d = 0.8$ | | | | $t/d = 0.5$ | | | |
|---|---|---|---|---|---|---|---|---|
| | SJ $\sigma_{tB}$ (MPa) | $15^o$ $\sigma_{tB}$ (MPa) | $30^o$ $\sigma_{tB}$ (MPa) | Flat $\sigma_{tB}$ (MPa) | SJ $\sigma_{tB}$ (MPa) | $15^o$ $\sigma_{tB}$ (MPa) | $30^o$ $\sigma_{tB}$ (MPa) | Flat $\sigma_{tB}$ (MPa) |
| Model 1 | 2.10 | 2.89 | 3.78 | 1.93 | 2.41 | 3.47 | 4.30 | 2.19 |
| Model 2 | 0.30 | 0.35 | 0.41 | 0.25 | 0.32 | 0.37 | 0.43 | 0.25 |
| Model 3 | 0.10 | 0.09 | 0.11 | 0.09 | 0.11 | 0.10 | 0.11 | 0.10 |

just before failure. To clarify the crack initiation of models shown in the figures, stresses at critical locations of maximum tension and compression are given in Table 5. The Model 1 under the loading condition of the flat platen showed crack initiation due to high compressive stress concentrations at the contact zone (Fig. 8). As models became more deformable, the compressive stress concentration decreased under the flat platens. Therefore, tensile cracking was initiated by stresses at the centers of discs under flat platen in the case of the Model 2 and Model 3.

High compressive stress regions were located beneath the edges of loading arcs with 15° contact (Fig. 10). According to the stress analyses, the crack initiation was found possible to occur at the contact zone of the discs having higher ratios of the tensile strength to compressive strength than those of the models. In particular, the compressive stresses had higher concentrations at the contact edges for the Model 1 which is the stiffest model. The compressive stress concentration at the edges decreased with an increase in contact angle for all the models. 30° loading arc simulations for all types of rock discs showed that the central stress distribution was much more effective for causing tensile crack initiation in comparison with 15° loading arc simulations. However, high contact angles caused an excessive load increase for crack occurrence. Table 6
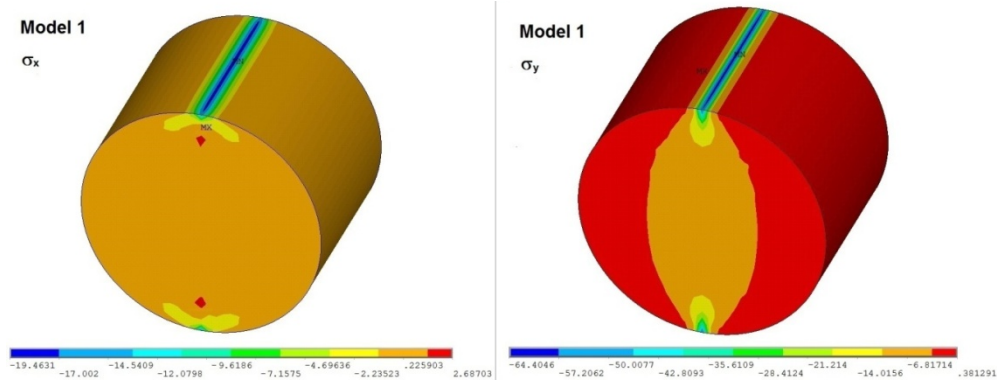
Fig. 8 Stress distribution in the Model 1 type disc under flat platens (+: tension, −: compression; blue: maximum compression, red: maximum tension; stresses are given in MPa)
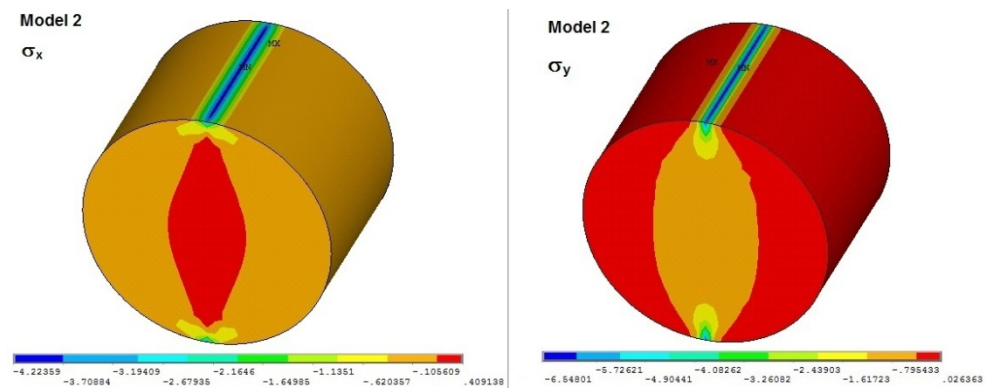


Fig. 9 Stress distribution in the Model 2 type disc under flat platens (+: tension, −: compression; blue: maximum compression, red: maximum tension; stresses are given in MPa)
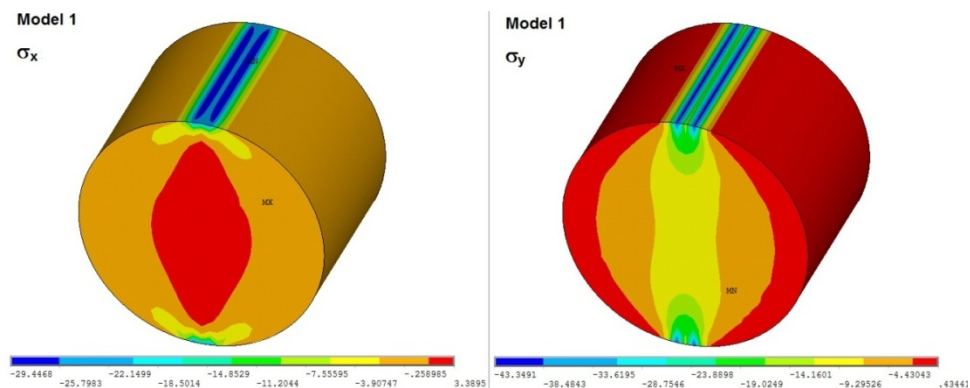


Fig. 10 Stress distribution in the Model 1 type disc under 15° loading arc (+: tension, −: compression; blue: maximum compression, red: maximum tension; stresses are given in MPa)
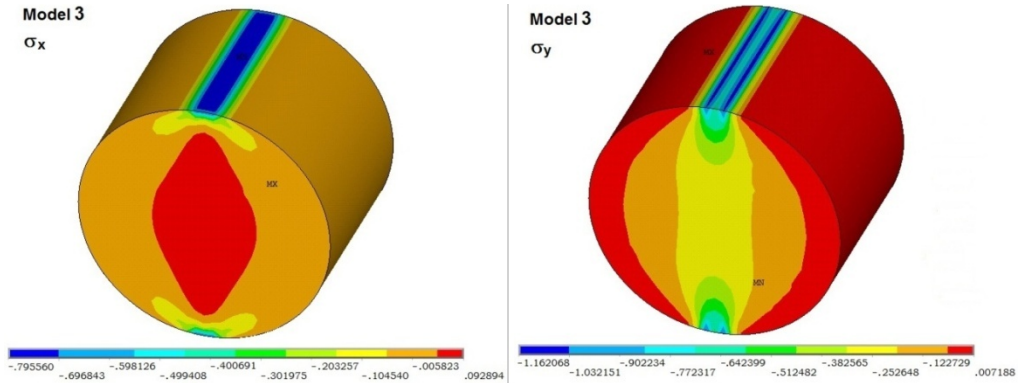
Fig. 11 Stress distribution in the Model 3 type disc under 15° loading arc (+: tension, −: compression; blue: maximum compression, red: maximum tension; stresses are given in MPa)



Fig. 12 Stress distribution in the Model 1 type disc under 30° loading arc (+: tension, −: compression; blue: maximum compression, red: maximum tension; stresses are given in MPa)
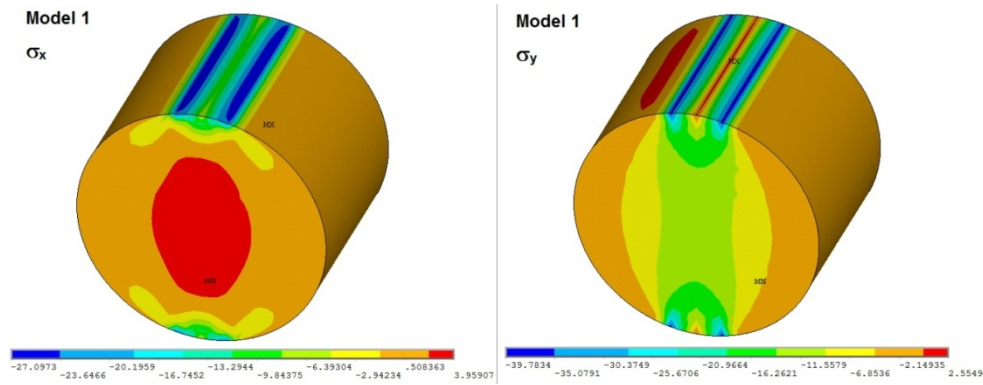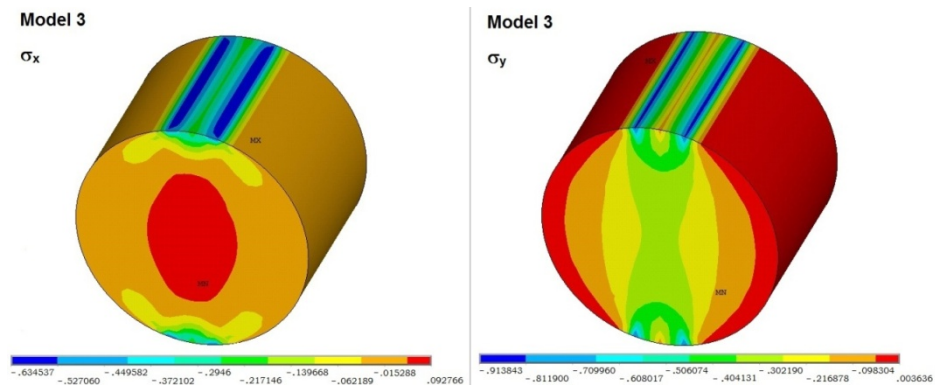


Fig. 13 Stress distribution in the Model 3 type disc under 30° loading arc (+: tension, −: compression; blue: maximum compression, red: maximum tension; stresses are given in MPa)
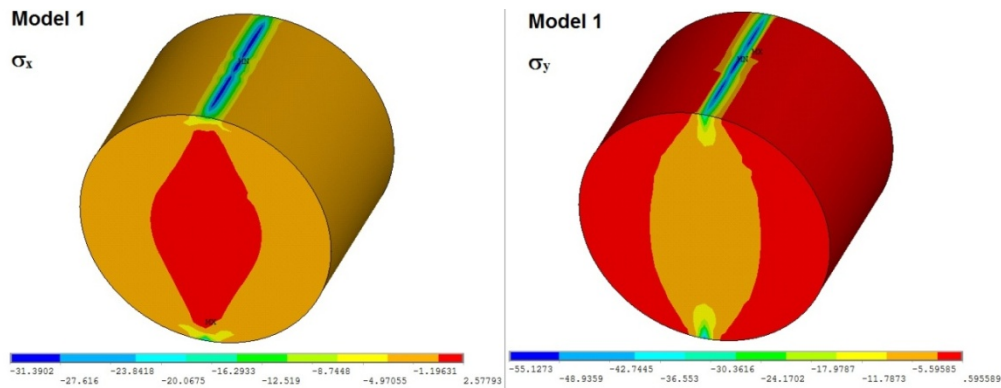
Fig. 14 Stress distribution in the Model 1 type disc under standard jaw (+: tension, −: compression; blue: maximum compression, red: maximum tension; stresses are given in MPa)
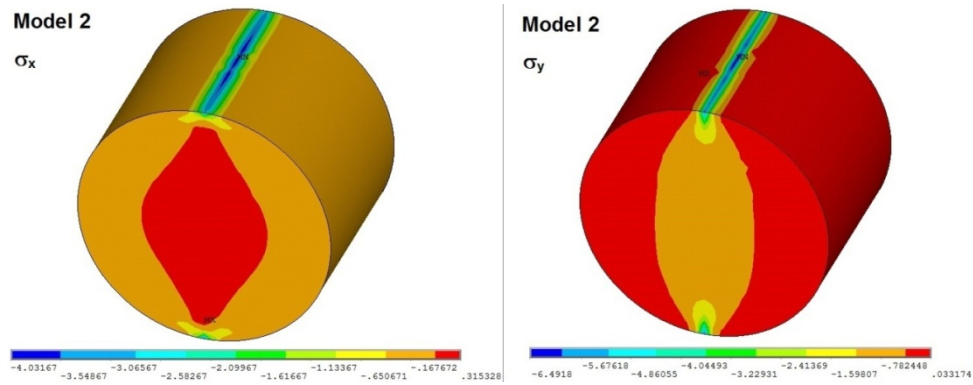


Fig. 15 Stress distribution in the Model 2 type disc under standard jaw (+: tension, −: compression; blue: maximum compression, red: maximum tension; stresses are given in MPa)

Table 6 Stresses for locations of maximum tension and compression (F: flat platen, 15: 15° loading arc, 30: 30° loading arc, SJ: standard jaw, R: radius of disc, r: distance from centre)

| Rock Model | Maximum tension | | | Maximum compression | | | Crack initiation |
|---|---|---|---|---|---|---|---|
| | Location | $\sigma_t$ (MPa) | $\sigma_c$ (MPa) | Location | $\sigma_1$ (MPa) | $\sigma_3$ (MPa) | |
| F-Model 1 | $r = 0.8$ R | 2.68 | -10.01 | Under platen | -64.40 | -19.46 | Under platen |
| F-Model 2 | Centre | 0.41 | -0.80 | Under platen | -6.55 | -4.22 | Centre |
| SJ-Model 1 | Centre | 2.58 | -5.60 | Under platen | -55.13 | -31.39 | Centre |
| SJ-Model 2 | Centre | 0.32 | -0.78 | Arc edges | -6.49 | -4.03 | Centre |
| 15-Model 1 | Centre | 3.39 | -9.30 | Arc edges | -43.35 | -29.45 | Centre |
| 15-Model 3 | Centre | 0.09 | -0.25 | Under platen | -1.16 | -0.80 | Centre |
| 30-Model 1 | Centre | 3.96 | -11.56 | Under platen | -39.78 | -27.10 | Centre |
| 30-Model 3 | Centre | 0.09 | -0.30 | Under platen | -0.91 | -0.63 | Centre |

gives the tensile strength values calculated in accordance with the first crack loads of the disc models.

Numerical simulation results for the flat platens confirmed the experimental findings in terms of fracturing behaviors of the disc specimens. The flat platens induced scattered cracks in the deformable soft materials, whereas cracking along the vertical diameter was obtained with the Model 1 which is the hardest model having the crack initiation in the contact zone.

Central crack initiation under the 30° loading arcs was confirmed by numerical modeling study. The boundary conditions of the loading arcs with definite contact angle differ from those of the standard jaw and flat platen. As the horizontal movement close to the contact zone between rock and loading arc is re-strained, the loading arcs cause high stress concentration just under the contact boundaries.

## 4. Discussions

Results of the experimental and numerical analyses were parallel in terms of the variations of ITS values, failing mechanism and crack shapes with the change of loading apparatus geometry and disc material deformability. According to the numerical analyses, the reason for the widely different ITS values of same paste backfill specimens tested in experimental study is confirmed to be significantly varied stress distribution in the discs under different loading conditions.

Komurlu and Kesimal (2015a) and Komurlu *et al*. (2015) applied ITS test on more than 200 disc specimens using the same loading apparatus with those used in this study and reported that the failure load increases with an increase in angle of loading arcs. The highest failure loads in the experiments applied on different kinds rock materials were generally obtained with 30° loading arcs. As parallel with the previous studies applied on rock materials, maximum ITS values for the paste backfill material with high cement ratio and high curing time were obtained with 30° loading arcs. However, paste backfill specimens with low cement ratio which are more deformable materials in comparison with the rock materials showed contrasting results. For the paste backfill specimens with low cement ratio, the standard Brazilian jaw and flat platens caused higher contact angles and ITS values in comparison with 30° and 15° loading arcs, respectively. ITS values of the discs loaded with 30° loading arcs were always higher than those obtained with 15° loading arcs. Because the standard jaw has higher contact angle than that of the flat platen, higher failure loads were obtained with the standard jaw in comparison with the flat platen.

The loading geometry and deformation characteristics of paste backfill specimens were found to be important factors in the determination of ITS. Both numerical study and experimental study results showing the dependency on the geometry of the loading apparatus confirmed the increase of ITS with an increase in contact angle. According to the numerical analyses, models of discs loaded with standard jaws and 30° loading arcs had higher failure loads than those of the discs loaded under flat platens and 15° loading arcs, respectively. The ratio between ITS values obtained with the standard jaw and the loading arcs was found to be dependent on the contact angle, disc deformability, load apparatus geometry and interaction with the disc.

The effect of friction between platens and discs was found to be important in terms of fracturing behavior of the disc specimens. Friction between the specimen and loading apparatus is dependent on the loading geometries and disc deformability (Markides *et al*. 2012, Kourkoulis *et al*. 2013, Markides and Kourkoulis 2013).

Another important outcome was obtained with the effect of thickness of the specimens on the ITS values of rocks. As same with previous studies, the ITS values reportedly decreased with an

increase in thickness of disc specimens (Yu *et al*. 2006, Komurlu and Kesimal 2012, 2015a, Komurlu *et al*. 2015).

Fracture toughness is an important tensile strength parameter of rocks. Erarslan and Williams (2012) reported that this value increases with an increase in loading arc angle. In this study, the fracture toughness was confirmed to decrease with a decrease in contact angle. The high differences between the loads of first crack initiation and failure were measured when the standard jaw and 30° loading arcs were used.

Many of the disc specimens shattered into several pieces under the standard Brazilian jaw. Because the standard formula considers a single splitting crack along the vertical diameter as an ideal split, the occurrence of scattered fracturing resulted in doubts about the mechanism of failure (Komurlu and Kesimal 2012, 2015a). Both experimental and numerical studies confirmed that crack shapes significantly varied with the change of disc material.

As a result of increasing modulus of elasticity of disc materials, stress concentration beneath the edges of loading arcs increased. Therefore, cracks branching toward the edges were observed in both experimental and numerical studies performed for stiff rocks under the 30° loading arc. In contrast, soft rock specimens failed with ideal central splitting without branching from the diametral plane. This observation is similar to the results of previous studies performed for Brisbane tuff (Erarslan *et al*. 2012, Erarslan and Williams 2012). However, very soft discs with low curing time and low cement ratio under 30° loading arcs were found to have a different failing with peripheral cracks out of the contact area.

New cracks can occur as a result of coalescence with the central crack and microcracks developed in the crushed region beneath contact area. Loading should be stopped when the first crack initiates. Otherwise, obtained failure loads would apparently differ between the first crack and final failure crack, and the ITS calculations would not be correct. Also, misleading ITS values can be obtained with excessive contact angles despite the first crack occurrence consideration. In numerical analyses, higher ITS values than the input parameter of uniaxial tensile strength were calculated by considering the crack initiation load of discs under 30° loading arcs. Because high contact area occurs at the contact of soft discs loaded with standard jaws, the Model 3 type of soft paste backfill disc model ITS calculated considering the first crack initiation was also higher than the input uniaxial tensile strength value of the model.

Stresses in the compression zone just beneath the load contact can be concluded to increase when the contact angle decreases. The first crack occurs in the contact region just beneath the platens in the case of disc failure initiated under the control of compressive stresses. Crack initiation at the contact zone caused smaller ITS in comparison with the central crack initiation.


## 5. Conclusions

The determination of ITS values was concluded to depend on the specimen material. A standard jaw should be used carefully to determine the ITS values of paste backfill by considering the disc material, deformation characteristics, toughness and failure shape. Standard jaw and flat platen which are the loading apparatus without a definite contact angle was not found convenient to represent the strength change resulting from the curing of paste backfill material. The change in the contact angle with an increase in curing time and having no definite contact angle were found to be important lackings causing undesirable misleading of determination of the ITS values of the cemented paste backfill materials.

Loading arcs with high contact angle of 30° and loading apparatus without a definite contact angle (standard jaw and flat platens) were found to have important disadvantages for being used in determination of the ITS values of the cemented paste backfill materials. Use of 15° loading arcs was found the most convenient way for the ITS tests of typical cemented paste backfill materials. However, the tests being applied by using the 15° loading arcs are recommended to carry out paying attention to be sure about the location of the crack initiation. A risk of crack initiation beneath the edges of the 15° loading arcs should be considered. With an increase in elasticity modulus resulting from an increase in the cement ratio and/or curing time, stress concentration at the contact zone edges under the loading arcs with definite contact angle was found to increase. To decrease the stress concentration at the contact zone and eliminate the risk of crack initiation under the control of compressive stresses induced under the edges of the loading arcs with 15° contact angle, further investigations for the possible use of 20° loading arcs are recommended.

## References

Akazawa, T. (1943), "New test method for evaluating internal stress due to compression of concrete (the splitting tension test) (part 1)", *J. Japan Soc. Civil Eng.*, **29**, 777-787.

Aono, Y., Tani, K., Okada, T. and Sakai, M. (2012), "Failure mechanism of the specimen in the splitting tensile strength test", *Proceedings of the 7th Asian Rock Mechanics Symposium*, Seoul, South Korea, October, pp. 615-623.

Ashour, H.A. (1988), "A compressive strength criterion for anisotropic rock materials", *Can. Geotech. J.*, **25**(2), 233-237.

Barla, G. and Innaurato, N. (1973), "Indirect tensile testing of anisotropic rocks", *Rock Mech. Rock Eng.*, **5**(4), 215-230.

Carneiro, F.L.L.B. (1943), "A new method to determine the tensile strength of concrete", *Proceedings of the 5th Meeting of the Brazilian Association for Technical Rules*, Brazil, September, pp. 126-129. [In Portuguese]

Chen, R. and Stimpson, B. (1993), "Interpretation of indirect tensile strength when moduli of deformation in compression and in tension are different", *Rock Mech. Rock Eng.*, **26**(2), 183-189.

Emad, M.Z., Mitri, H. and Kelly C. (2015), "State-of-the-art review of backfill practices for sublevel stoping system", *Int. J. Min. Reclam. Environ.*, **29**(6), 544-556. DOI: 10.1080/17480930.2014.889363

Erarslan, N. and Williams, D.J. (2012), "Experimental, numerical and analytical studies on tensile strength of rocks", *Int. J. Rock Mech. Min. Sci.*, **49**, 21-30.

Erarslan, N., Liang, Z.Z. and Williams. D.J. (2012), "Experimental and Numerical Studies on Determination of Indirect Tensile Strength of Rocks", *Rock Mech. Rock Eng.*, **45**(5), 739-751.

Fairbairn, E.M.R. and Ulm, J.F. (2002), "A tribute to Fernando L.L.B. Carneiro (1913-2001) Engineer and Scientist who invented the Brazilian Test", *Mater. Struct.*, **35**, 195-196.

Fairhurst, C. (1964), "On the validity of the 'Brazilian' test for brittle materials", *Int. J. Rock Mech. Min. Sci.*, **1**(4), 535-546.

Hobbs, D.W. (1964), "The tensile strength of rocks", *Int. J. Rock Mech. Min. Sci.*, **1**(3), 385-396.

Hondros, G. (1959), "The evaluation of Poisson's ratio and the modulus of materials of a low tensile resistance by Brazilian (indirect tensile) test with particular reference to concrete", *Aust. J. Appl. Sci.*, **10**(3), 243-268.

ISRM (1978), "International society for rock mechanics suggested methods for determining tensile strength of rock materials", *Int. J. Rock Mech. Min. Sci. Geomech. Abstr.*, **15**, 99-103.

Jaeger, J.C. and Cook, N.G.W. (1976), *Fundamentals of Rock Mechanics*, Chapman and Hall, London, UK.

Jianhong, Y. and Wu, F.Q. and Sun, J.Z. (2009), "Estimation of the tensile elastic modulus using Brazilian disc by applying diametrically opposed concentrated loads", *Int. J. Rock Mech. Min. Sci.*, **46**(3), 568-576.

Kesimal, A., Yilmaz, E. and Ercikdi, B. (2004), "Evaluation of paste backfill mixtures consisting of

sulphide-rich mill tailings and varying cement contents", *Cement Concrete Res*, **34**(10), 1817-1822.

Komurlu, E. and Kesimal, A. (2012), "Jaw effects on indirect tensile strength test disc failure mechanism", *Proceedings of the 7th Asian Rock Mechanics Symposium*, Seoul, South Korea, October, pp. 624-637.

Komurlu, E. and Kesimal, A. (2015a), "Evaluation of indirect tensile strength of rocks using different types of jaws", *Rock Mech. Rock Eng.*, **48**(4), 1723-1730.

Komurlu, E. and Kesimal, A. (2015b), "Sulfide-rich mine tailings usage for short-term support purposes: An experimental study on paste backfill barricades", *Geomech. Eng., Int. J.*, **9**(2), 195-205.

Komurlu, E., Kesimal, A. and Ercikdi, B. (2013), "An investigation of uncemented paste backfill applicability", *Proceedings of the 23th International Congress and Exhibition of Tukey (IMCET 2013)*, The Chamber of Mining Engineers of Turkey, Antalya, Turkey, April, pp. 1017-1024

Komurlu, E., Kesimal, A. and Demir, S. (2015), "An experimental and numerical study on determination of indirect (Splitting) tensile strength of rocks under various load apparatus", *Can. Geotech. J.*, **53**(2), 360-372. DOI: 10.1139/cgj-2014-0356

Kourkoulis, S.K. and Markides, C.F. (2012), "The Brazilian disc under parabolically varying load: Theoretical and experimental study of the displacement field", *Int. J. Solid. Struct.*, **49**(7-8), 959-972.

Kourkoulis, S.K., Markides, C.F. and Hemsley, J.A. (2013), "Frictional stresses at the disc-jaw interface during the standardized execution of the Brazilian disc test", *Acta Mechanica*, **224**(2), 255-268.

Krishnayya, A.V.G. and Eisenstein, Z. (1974), "Brazilian tensile test for soils", *Can. Geotech. J.*, **11**(4), 632-642.

Li, L. and Aubertin, M. (2002), "A crack-induced stress approach to describe the tensile strength of transversely isotropic rocks", *Can. Geotech. J.*, **39**(1), 1-13.

Markides, C.F. and Kourkoulis, S.K. (2013), "Naturally accepted boundary conditions for the Brazilian Disc Test and the corresponding stress field", *Rock Mech. Rock Eng.*, **46**(5), 959-980.

Markides, C.F., Pazis, D.N. and Kourkoulis, S.K. (2010), "Closed Full-Field Solutions for Stresses and Displacements in the Brazilian Disc under Distributed Radial Load", *Int. J. Rock Mech. Min. Sci.*, **47**(2), 227-237.

Markides, C.F., Pazis, D.N. and Kourkoulis, S.K. (2012), "The Brazilian disc under non-uniform distribution of radial pressure and friction", *Int. J. Rock Mech. Min. Sci.*, **50**, 47-55.

Muskhelishvili, N.I. (1963), *Some Basic Problems in Mathematical Theory of Elasticity*, Noordhoff International Publishing, Leyden, IL, USA.

Ulusay, R. and Gokceoglu, C. (1997), "The modified block punch index test", *Can. Geotech. J.*, **34**(6), 991-1001.

Ulusay, R. and Hudson, J.A. (Eds.) (2007), *The Blue Book - The Complete ISRM Suggested Methods for Rock Characterisation, Testing and Monitoring: 1974-2006*, ISRM & Turkish National Group of ISRM, Ankara, Turkey.

Willam, K.J. and Warnke, E.P. (1974), *Constitutive Model for the Triaxial Behaviour of Concrete*, IABSE, Report No. 19; Bergamo, Italy, pp. 1-30.

Yilmaz, E., Belem, T., Bussiere, B. and Benzaazoua, M. (2011), "Relationships between microstructural properties and compressive strength of consolidated and unconsolidated cemented paste backfills", *Cement Concrete Compos.*, **33**(6), 702-715.

Yilmaz, E., Belem, T. and Benzaazoua, M. (2015), "Specimen size effect on strength behavior of cemented paste backfills subjected to different placement conditions", *Eng. Geol.*, **185**, 52-62.

Yu, Y., Yin, J. and Zhong, Z. (2006), "Shape effects in the Brazilian tensile strength test and a 3D FEM correction", *Int. J. Rock Mech. Min. Sci.*, **43**(4), 623-627.

*JS*